


Nematic heavy fermions and coexisting magnetic order in CeSiI

Aayush Vijayvargia  and Onur Erten

Department of Physics, Arizona State University, Tempe, Arizona 85287, USA



(Received 19 February 2024; accepted 1 May 2024; published 16 May 2024)

Motivated by the recent discovery of magnetism and heavy quasiparticles in the van der Waals material CeSiI, we develop an effective model that incorporates the conduction electrons residing at the silicene layer interacting with the local moments of the Ce ions. Ce sites are arranged on two layers of triangular lattices, above and below the silicene layer, and they are located at the center of the honeycomb lattice. This arrangement results in an effective extended Kondo interaction along with a predominant ferromagnetic Ruderman-Kittel-Kasuya-Yosida interaction. Via the mean-field theory of Abrikosov fermions, our analysis indicates that the ground state of the monolayer can exhibit a nonmagnetic nematic heavy fermion phase that breaks C_6 rotational symmetry for a small Heisenberg exchange and a magnetically ordered phase for a large Heisenberg exchange. For intermediate values, a coexistence of magnetic order and a uniform heavy Fermi liquid is stabilized where they reside on separate Ce layers. We show that this phase can further be enhanced by an external electric field. Our results provide a natural mechanism for the coexistence of magnetic order and heavy fermions in CeSiI and highlight the possibility of unconventional nonmagnetic heavy fermions with broken rotational symmetry.

DOI: [10.1103/PhysRevB.109.L201118](https://doi.org/10.1103/PhysRevB.109.L201118)

Introduction. Heavy fermions are an archetypical class of strongly correlated materials that possess local moments, generally originating from lanthanide or actinide ions, interacting with conduction electrons via an antiferromagnetic Kondo interaction [1–3]. They host an array of exotic phenomena including unconventional superconductivity, hidden order, and strange metals [4–6]. Most heavy fermion materials are intermetallics and exhibit strong chemical bonding along all directions which prevent the isolation of two-dimensional (2D) monolayers. In contrast, the recent discovery of magnetism and 2D heavy quasiparticles in CeSiI [7,8] provides a rare example of a van der Waals (vdW) heavy fermion platform. 2D vdW materials are highly tunable systems that can be controlled via strain, gating, and electric field [9]. Furthermore, they can be arranged in different stacking patterns and twisted to form moiré superlattices which can give rise to even richer phenomena that may not be possible to realize in monolayers [10]. Therefore, introducing heavy fermions to 2D materials adds another dimension to the list of phenomena, functionalities, and the potential for vertical integration in vdW heterostructures.

CeSiI orders magnetically at $T_c = 7.5$ K. Neutron scattering experiments [7] show that the ordering wave vector is $\mathbf{q} = (0.28, 0, 0.19)$, resulting in a spiral ground state with a long wavelength, $\lambda = 2\pi/q_a \sim 22$ unit cells, considering a monolayer. Furthermore, the Sommerfeld coefficient of CeSiI, $\gamma_{\text{CeSiI}} = 0.125 \text{ J mol}^{-1} \text{ K}^{-2}$, shows significant enhancement compared to its nonmagnetic analog LaSiI, $\gamma_{\text{LaSiI}} = 0.003 \text{ J mol}^{-1} \text{ K}^{-2}$, indicating the formation of heavy fermions [8]. The temperature dependence of resistivity, the Fano shape of the tunneling spectrum, and the angle-resolved photoemission spectroscopy experiments further corroborate the existence of heavy quasiparticles [8].

Motivated by these advancements, we develop an effective model for a monolayer CeSiI that involves the conduction

electrons at the silicene layer—a honeycomb lattice formed by Si atoms—and the local moments at the Ce sites. Ce ions form two layers of triangular lattices that sandwich the silicene layer. Each Ce site sits at the center of the honeycomb lattice and couples to six nearest-neighbor (NN) conduction electron sites as depicted in Fig. 1. We solve this model with the extended Kondo interactions using the mean-field theory of Abrikosov fermions. Our main results are as follows: (i) Since both Ce layers couple to the conduction electrons via the same form factor, a uniform heavy fermion state only screens the symmetric superposition of the local moments on each layer while the antisymmetric superposition remains unscreened. This results in an unstable phase with flat bands at the chemical potential. (ii) Via a nonrestrictive mean-field ansatz, we find that the channel symmetry can be spontaneously broken and two types of heavy fermion phases can be stabilized. The first one is a nonmagnetic phase where local moments on layer 1 (2) couple primarily to the silicene sublattice A (B) as depicted in Fig. 2(b). This phase preserves inversion symmetry but breaks mirror reflection and C_6 rotational symmetry and thus exhibits a nematic order parameter. The second phase breaks the channel symmetry by ordering magnetically on one layer and forming a uniform heavy fermion on the other layer, resulting in a coexistence similar to experimental observations. For a large Heisenberg interaction, both layers order magnetically. (iii) We show that the stability of the coexistent phase can be enhanced further via the application of an external electric field.

The rest of the Letter is organized as follows. We introduce the model, discuss the origin of the ferromagnetic (FM) nearest-neighbor (NN) exchange, and describe the methodology including the mean-field theory. Then, we present our results for different parameter regimes. Finally, we conclude with a summary of our results and an outlook.

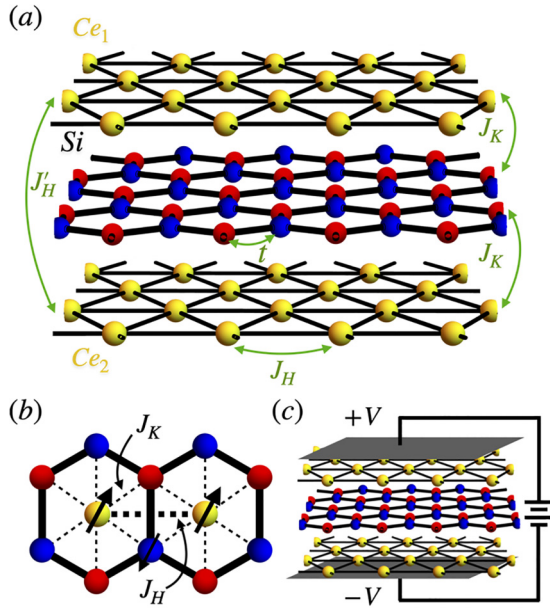


FIG. 1. (a) Schematic of the model: Ce sites (yellow) form two layers of triangular lattice. The silicene layer—a honeycomb lattice formed by Si atoms (red and blue for the A and B sublattice)—is sandwiched between the Ce layers. The arrows indicate the interaction terms in our model including the Kondo interaction (J_K) between the local moments and the conduction electrons as well as the intra- (J_H) and interlayer (J'_H) Heisenberg exchange between the local moments. Iodine layers do not play a significant role in the low-energy model and therefore they are omitted on the schematic. (b) Top view of the model that shows the local moment interacting with six conduction electron sites via the Kondo interaction. (c) Electric field tuning of the monolayer: Applying the $+V$, $-V$ potential shifts the energy levels of the Ce layers, increasing the Kondo coupling on one layer while decreasing on the other. The electric field does not affect the chemical potential of the conduction electrons.

Model and methods. The first-principles calculations suggest that the conduction electrons primarily occupy the silicene bands [11,12]. These bands are self-doped by the Ce d electrons, shifting the chemical potential far from the Dirac point. We consider a model where the Ce local moments on layer 1, 2 couple to the conduction electrons at six silicene sites via the Kondo interaction. While the Kondo interaction generates a Ruderman-Kittel-Kasuya-Yosida (RKKY) term that can induce magnetic order, this is not captured within the Abrikosov fermion mean-field theory that we employ. In order to proxy the RKKY coupling, we consider FM intra- and interlayer Heisenberg interactions among the local moments. The Hamiltonian reads

$$\begin{aligned}
H = & -t \sum_{(ij)\sigma} (c_{iA\sigma}^\dagger c_{jB\sigma} + \text{H.c.}) - \mu \sum_{i\sigma s} c_{i\sigma s}^\dagger c_{i\sigma s} \\
& + \sum_{i,\delta,\nu} J_K^\nu \sigma_{fiv} \cdot \sigma_{c(i+\delta)} - J_H \sum_{(ij)\nu} \sigma_{fiv} \cdot \sigma_{fj\nu} \\
& - J'_H \sum_i \sigma_{fi1} \cdot \sigma_{fi2},
\end{aligned} \quad (1)$$

where $\nu = 1, 2$ is the Ce layer index, $s = A, B$ represent the silicene sublattice, and δ denotes the six nearest Ce-Si

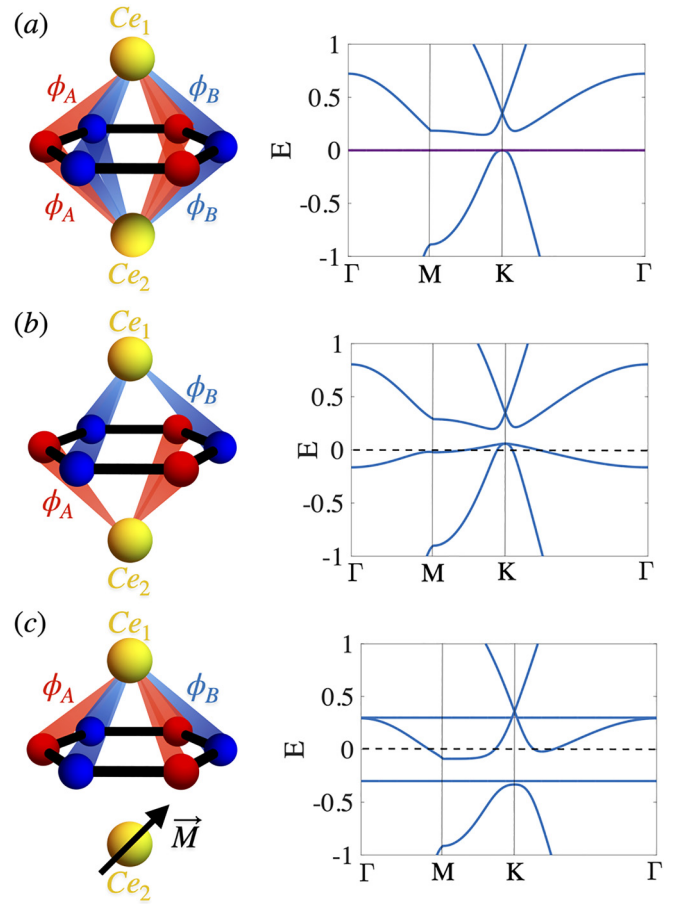


FIG. 2. Schematic of different phases and the corresponding excitation spectra: (a) A uniform HFL phase where all ϕ 's are equal. This phase has flat bands at zero energy and therefore it is unstable. (b) A nematic heavy Fermi liquid where local moments in layer 1 primarily couple to one sublattice whereas the layer 2 couples to the other sublattice. (c) A coexistence of magnetic order and a uniform heavy Fermi liquid.

neighbors. c^\dagger and $\sigma_{c(f)}$ are the creation and spin operators of the conduction electrons (local moments). $J_K^{1(2)}$ is the Kondo coupling in layer 1(2), J_H and J'_H are the intra- and interlayer Heisenberg exchanges, respectively. Equation (1) can be derived from a Schrieffer-Wolff transformation of the periodic Anderson model [13]. Note that this procedure gives rise to additional terms such as a correlated hopping combined with a spin flip [14]. However, we are restricting our analysis only to the spin-spin interactions. Note that the extended Kondo interaction is crucial to obtain topological phases in heavy fermion systems [15–18]. It has also been investigated in the context of d -wave heavy fermions [19,20] and unusual magnetic interactions [21].

The spiral ground state of CeSiI with a long wavelength, $\lambda \sim 22a$, indicates that the angle between the magnetic moments within a unit cell is quite small ($\Delta\theta \sim 16^\circ$) and locally, they can approximately be considered FM. One of the simplest ways to generate such a spiral is to consider a spin Hamiltonian with a large FM NN exchange (J_1) and a weak antiferromagnetic (AFM) next-nearest-neighbor (NNN) exchange (J_2). Performing a Luttinger-Tisza analysis [22] on

the $J_1 - J_2$ Hamiltonian results in $H = \sum_{\mathbf{q}} J(\mathbf{q}) S_{\mathbf{q}} S_{-\mathbf{q}}$, where $J(\mathbf{q}) = -J_1 \sum_{\Delta} \cos \mathbf{q} \cdot \Delta + J_2 \sum_{\Delta'} \cos \mathbf{q} \cdot \Delta'$, where we sum over Δ and Δ' which are the NN and NNN vectors, respectively. For $J_2/J_1 \simeq -0.11$, it is possible to obtain a spiral ground state with \mathbf{q} that is similar to the experimental value. For the remainder of this Letter, we only consider a FM NN Heisenberg exchange to avoid the intricacies arising from a large unit cell.

Next, we describe the mean-field approach. We begin by representing the local moment spins in terms of Abrikosov fermions [23–26]: $\sigma_{fiv} = f_{iv\sigma}^\dagger \sigma_{\sigma\sigma'} f_{iv\sigma'}$, subject to the constraint $\sum_{\sigma} f_{iv\sigma}^\dagger f_{iv\sigma} = 1$. We decouple the Kondo interaction term in the hybridization channel, $(f_{iv\alpha}^\dagger \sigma_{\alpha\beta} f_{iv\beta})(c_{i+\delta\alpha'}^\dagger \sigma_{\alpha'\beta'} c_{i+\delta\beta'}) = -2(f_{iv\alpha}^\dagger c_{i+\delta\alpha})(c_{i+\delta\beta}^\dagger f_{iv\beta}) \approx \sum_s \phi_{vs} (\sum_{\delta_s} c_{i+\delta_s s}^\dagger) f_{iv\sigma} + \text{H.c.}$, where $s = A, B$, and δ_s are vectors connecting the center of the hexagon to the s sublattice. The Kondo hybridization is $\phi_{vs} = \langle f_{iv\sigma}^\dagger (\sum_{\delta_s} c_{i+\delta_s s}) \rangle / 3 = \langle \Gamma_s(k) f_{kv\sigma}^\dagger c_{ks\sigma} \rangle / 3$, where $\Gamma_s(k) = \sum_{\delta_s} e^{ik \cdot \delta_s}$. We decouple the Heisenberg interaction $\sigma_{fiv}^\alpha \sigma_{fjv}^\alpha = M^\alpha \sigma_{fjv}^\alpha + M^\alpha \sigma_{fiv}^\alpha$ where $M_v^\alpha = \langle \sigma_{fiv}^\alpha \rangle = \langle f_{iv}^\dagger \sigma^\alpha f_{iv} \rangle$. The mean-field Hamiltonian reads

$$\begin{aligned} H_{\text{MF}} = & -t \sum_{k\sigma} (c_{kA\sigma}^\dagger c_{kB\sigma} + \text{H.c.}) - \mu \sum_{k\sigma s} c_{ks\sigma}^\dagger c_{ks\sigma} \\ & - \sum_{k,v} 2J_K^v \sum_s \phi_{vs} \Gamma_s^*(k) c_{ks\sigma}^\dagger f_{kv\sigma} + \text{H.c.} \\ & - 3J_H \sum_{kv} \mathbf{M}_v \cdot (f_{kv}^\dagger \sigma f_{kv}) \\ & - J'_H \sum_{kv} \mathbf{M}_1 \cdot (f_{k2}^\dagger \sigma f_{k2}) + \mathbf{M}_2 \cdot (f_{k1}^\dagger \sigma f_{k1}) \\ & - \sum_{kv\sigma} \lambda_v (f_{kv\sigma}^\dagger f_{kv\sigma} - 1). \end{aligned} \quad (2)$$

We estimate the mean-field order parameters $\{\phi_{1A}, \phi_{1B}, \phi_{2A}, \phi_{2B}, \mathbf{M}_1, \mathbf{M}_2\}$ and the Lagrange multipliers $\{\lambda_1, \lambda_2\}$ self-consistently. For the remainder of this Letter we fix $J_K^v/t = 0.65$ (the bandwidth is $6t$) and the chemical potential μ sufficiently away from the Dirac points, resulting in $n_c = \sum_{i\sigma} c_{i\sigma}^\dagger c_{i\sigma} = 0.82$.

Apart from the ground state phase diagram, we also explore the effects of electric field tuning. We consider a setup where $+V$ and $-V$ voltages are applied by top and bottom gates. This does not affect the chemical potential of the silicene layer. However, the energy levels of the local moments on layer 1(2), $\epsilon_{f1(2)}$, increase (decrease) with respect to the chemical potential due to the potential drop, $\epsilon_{f1/2} \rightarrow \epsilon_{f1/2} \mp e\Delta V$. Since Ce ions primarily fluctuate via $f^1 \leftrightarrow f^0$, the Kondo exchange on two layers gets modified as follows, $J_K^{1/2} = t_{cf}^2 / (\epsilon_f \mp e\Delta V) = J_{K0} / (1 \mp e\Delta V / \epsilon_f)$, where $J_{K0} = t_{cf}^2 / \epsilon_f$ is the Kondo coupling in the absence of an external electric field.

Results and discussion. There are two key ingredients in our model that differentiate it from a standard Kondo-Heisenberg model. The first one is the extended Kondo exchange where each local moment couples to six conduction electrons. The second is the presence of two layers of local moments that couple to the conduction electrons via the same form factor. To illustrate the impact of the latter, we consider

our model with only a single layer of local moments. Our mean-field analysis shows that a uniform heavy Fermi liquid (HFL) forms with $\phi_A = \phi_B$ and $\mathbf{M} = 0$ for small J_H/J_K . A first-order transition to a magnetically ordered state takes place at $J_H/J_K = 0.52$. Similar behavior has been observed in other Kondo-Heisenberg type models [26]. Note that the uniform HFL has the same ϕ for all six bonds and carry zero magnetization whereas the magnetically ordered phase has $\phi = 0$ for all bonds. In the large J_K limit of this model, a Kondo insulator will not be observed when the conduction band is half filled. The reason for this can be attributed to the mismatch in the number of electrons. The number of conduction electrons at half filling is twice the number of local moments. Hence, even after all local moments form singlets, the residual conduction electrons will prevent the Kondo insulator phase.

Proceeding with the original model with two layers of local moments, we recognize that a uniform HFL with $\phi_{1A} = \phi_{1B} = \phi_{2A} = \phi_{2B}$ is not attainable in this case. As shown in Fig. 2(a), a uniform HFL has doubly degenerate flat f bands at zero energy. This phase is unstable to perturbations and cannot be the ground state. To elucidate the origin of the flat bands, we perform a rotation to a basis with the symmetric and antisymmetric linear combinations of the f fermions as $f_{p\sigma}^\dagger = (f_{1\sigma}^\dagger + f_{2\sigma}^\dagger) / \sqrt{2}$ and $f_{m\sigma}^\dagger = (f_{1\sigma}^\dagger - f_{2\sigma}^\dagger) / \sqrt{2}$. For uniform HFL with equal ϕ 's for all bonds, it is clear that in Eq. (2) only the symmetric linear combination couples to the conduction electrons whereas the antisymmetric combination remains unscreened, resulting in flat bands at $E = 0$. Therefore, the uniform HFL solution shows a resemblance to an underscreened Kondo model where the conduction electrons are unable to screen all of the local moments [27]. However, we note that there are exactly two local moments and two conduction electron site per unit cell and thus our model should not be underscreened. This paradox arises due to the fact that the local moments on layer 1 and 2 couple to the conduction electrons with the same form factor (equal ϕ 's). Accordingly, only a linear combination of them gets screened. To overcome this issue, we perform unrestricted mean-field calculations where we allow $\{\phi_{1A}, \phi_{1B}, \phi_{2A}, \phi_{2B}\}$ to be different from each other in order to break the channel symmetry between the layers. We obtain two nonuniform HFL phases: (i) a nonmagnetic nematic HFL and (ii) a coexistence of a uniform HFL on one layer and magnetic order on the other layer.

Nematic heavy Fermi liquid. As depicted in Fig. 2(b), in this phase the local moments in layer 1 couple primarily to one sublattice whereas layer 2 couples to the other sublattice, such as $\phi_{1B} = \phi_{2A} \gg \phi_{1A} = \phi_{2B}$. This phase preserves the inversion symmetry whereas it breaks sublattice, mirror reflection, and C_6 rotational symmetry. Consequently, it exhibits a nematic order parameter. Nematic HFL was first proposed by Ref. [28] in the context of chiral spin liquids hybridizing with metals. However, in our model it is generated self-consistently. Since nematic HFL breaks point group symmetries, it exhibits a Ginzburg-Landau type phase transition with T_c set by the Kondo temperature. It is one of the rare examples of a phase transition driven by the Kondo effect and in that sense it is similar to hastatic order [29] and Kondo stripe order [30].

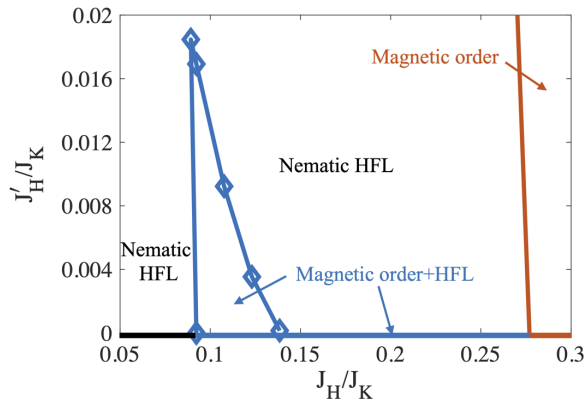


FIG. 3. Ground state phase diagram as a function of J_H/J_K and J'_H/J_K . We obtain a nonmagnetic nematic HFL, a coexisting magnetic order and HFL, and a magnetic order on both layers. All of the phase transitions are first order.

Coexistence of magnetic order and HFL. This phase breaks the channel symmetry by ordering magnetically on one layer and forming a uniform HFL on the other layer such as $\phi_{1A} = \phi_{1B} \neq 0$, $\phi_{2A} = \phi_{2B} = 0$ as depicted in Fig. 2(c). Unlike spin density wave type magnetism observed in heavy fermions such as $\text{Ce}_3\text{Pd}_{20}\text{Si}_6$ [31], the coexisting phase in our model has a clear phase separation in real space. A similar separation of magnetic order and heavy quasiparticles has been observed in modulated magnetic textures in CeRhIn_5 [32], CeAuSb_2 [33], and also in CeSb but in momentum space [34].

In Fig. 3, we present the ground state phase diagram as a function of J_H/J_K and J'_H/J_K . For $J'_H = 0$, the ground state evolves from a nematic HFL to a coexisting magnetic order and HFL to a polarized magnetic phase as a function of J_H . For a small interlayer Heisenberg interaction J'_H the nematic HFL is unaffected. On the contrary, for the coexistence phase, J'_H acts as a static magnetic field for the HFL and destabilizes it quite rapidly. All of the phase transitions are first order and are determined by the energy crossings of the corresponding phases. In the large J_K limit, a Kondo insulator would be observed at half filling of the conduction band. There are two electrons in the conduction band and two local moments per unit cell. Consequently, singlet formation at large J_K will allow for a Kondo insulator phase. However, in our calculations we do not observe this Kondo insulator phase as $\Gamma(k)$ vanishes at the Dirac point. This prevents a gap from opening when the conduction band is half filled, accordingly no Kondo insulator is observed.

Next, we discuss the electric field tuning of the phase diagram. As described above, the external electric field modifies the Kondo coupling on two layers as $J_K^{1/2} = J_{K0}/(1 \mp e\Delta V/\epsilon_f)$ while maintaining the same chemical potential for the conduction electrons. As shown in Fig. 4, an electric field enhances the stability of the coexistence of magnetic

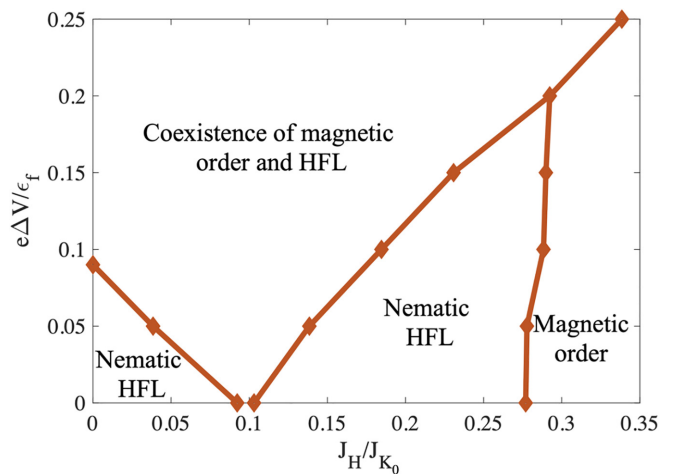


FIG. 4. Effects field tuning of the phase diagram for $J'_H/J_K = 0.01$: Electric field shifts the energy levels of the local moments and therefore increases the Kondo interaction on one layer while decreasing it on the other layer. This significantly enhances the stability of the coexistence of magnetic order and HFL.

order and HFL over the other phases. This is due to the fact that increasing the Kondo coupling on the layer where the HFL resides lowers the energy whereas decreasing the Kondo coupling on the magnetic layer does not impact the energy. In total, the energy of the coexistent phase decreases significantly. Conversely, the nematic HFL has finite hybridization on both layers, and the modification of the Kondo couplings approximately cancel each other and the energy is not affected in significant manner.

There are several key experimental signatures of the nonuniform heavy fermion phases that we predict. For instance, NMR experiments can distinguish if the magnetic order is uniform or if there is a phase separation of magnetism and HFL on different layers. Regarding the nematic HFL, C_6 symmetry breaking can be deduced from angle-dependent transport, Raman spectroscopy, as well as the finite-temperature phase transition.

Conclusions. We constructed a low-energy model for the vdW heavy fermion material CeSiI and studied its phase diagram via mean-field theory. We showed that the unique geometry of the interactions prevents a uniform HFL. In return, we showed that a nematic HFL or a coexistence of magnetic order and HFL can be stabilized. In particular, the coexistent phase can be further enhanced by the application of an external electric field. Interesting future directions include heterostructures involving CeSiI and its moiré superlattices.

Acknowledgment. We thank Filip Ronning, Piers Coleman, Emilian Nica, and Turan Birol for fruitful discussions. This work is supported by NSF Award No. DMR-2234352.

- [1] G. R. Stewart, Heavy-fermion systems, *Rev. Mod. Phys.* **56**, 755 (1984).
- [2] S. Wirth and F. Steglich, Exploring heavy fermions from macroscopic to microscopic length scales, *Nat. Rev. Mater.* **1**, 16051 (2016).

- [3] P. Coleman, *Introduction to Many-Body Physics* (Cambridge University Press, Cambridge, UK, 2015).
- [4] B. White, J. Thompson, and M. Maple, Unconventional superconductivity in heavy-fermion compounds, *Phys. C: Supercond. Appl.* **514**, 246 (2015).

- [5] J. A. Mydosh, P. M. Oppeneer, and P. S. Riseborough, Hidden order and beyond: An experimental–theoretical overview of the multifaceted behavior of URu₂Si₂, *J. Phys.: Condens. Matter* **32**, 143002 (2020).
- [6] P. Coleman, C. Pépin, Q. Si, and R. Ramazashvili, How do Fermi liquids get heavy and die?, *J. Phys.: Condens. Matter* **13**, R723 (2001).
- [7] R. Okuma, C. Ritter, G. J. Nilsen, and Y. Okada, Magnetic frustration in a van der Waals metal CeSiI, *Phys. Rev. Mater.* **5**, L121401 (2021).
- [8] V. A. Posey, S. Turkel, M. Rezaee, A. Devarakonda, A. K. Kundu, C. S. Ong, M. Thinel, D. G. Chica, R. A. Vitalone, R. Jing, S. Xu, D. R. Needell, E. Meirzadeh, M. L. Feuer, A. Jindal, X. Cui, T. Valla, P. Thunström, T. Yilmaz, E. Vescovo *et al.*, Two-dimensional heavy fermions in the van der Waals metal CeSiI, *Nature (London)* **625**, 483 (2024).
- [9] Y. Liu, N. O. Weiss, X. Duan, H.-C. Cheng, Y. Huang, and X. Duan, Van der Waals heterostructures and devices, *Nat. Rev. Mater.* **1**, 16042 (2016).
- [10] F. He, Y. Zhou, Z. Ye, S.-H. Cho, J. Jeong, X. Meng, and Y. Wang, Moiré patterns in 2D materials: A review, *ACS Nano* **15**, 5944 (2021).
- [11] B. G. Jang, C. Lee, J.-X. Zhu, and J. H. Shim, Exploring two-dimensional van der Waals heavy-fermion material: Data mining theoretical approach, *npj 2D Mater. Appl.* **6**, 80 (2022).
- [12] A. O. Fumega and J. L. Lado, Nature of the unconventional heavy-fermion Kondo state in monolayer CeSiI, *Nano Lett.* **24**, 4272 (2024).
- [13] J. R. Schrieffer and P. A. Wolff, Relation between the anderson and Kondo Hamiltonians, *Phys. Rev.* **149**, 491 (1966).
- [14] V. Alexandrov and P. Coleman, End states in a one-dimensional topological Kondo insulator in large-*N* limit, *Phys. Rev. B* **90**, 115147 (2014).
- [15] M. Dzero, J. Xia, V. Galitski, and P. Coleman, Topological Kondo insulators, *Annu. Rev. Condens. Matter Phys.* **7**, 249 (2016).
- [16] V. Alexandrov, P. Coleman, and O. Erten, Kondo breakdown in topological Kondo insulators, *Phys. Rev. Lett.* **114**, 177202 (2015).
- [17] A. Ghazaryan, E. M. Nica, O. Erten, and P. Ghaemi, Shadow surface states in topological Kondo insulators, *New J. Phys.* **23**, 123042 (2021).
- [18] H.-H. Lai, S. E. Grefe, S. Paschen, and Q. Si, Weyl-Kondo semimetal in heavy-fermion systems, *Proc. Natl. Acad. Sci. USA* **115**, 93 (2018).
- [19] P. Ghaemi and T. Senthil, Higher angular momentum Kondo liquids, *Phys. Rev. B* **75**, 144412 (2007).
- [20] P. Ghaemi, T. Senthil, and P. Coleman, Angle-dependent quasi-particle weights in correlated metals, *Phys. Rev. B* **77**, 245108 (2008).
- [21] S. Ahamed, R. Moessner, and O. Erten, Why rare-earth ferromagnets are so rare: Insights from the *p*-wave Kondo model, *Phys. Rev. B* **98**, 054420 (2018).
- [22] J. M. Luttinger and L. Tisza, Theory of dipole interaction in crystals, *Phys. Rev.* **70**, 954 (1946).
- [23] P. Coleman and N. Andrei, Kondo-stabilised spin liquids and heavy fermion superconductivity, *J. Phys.: Condens. Matter* **1**, 4057 (1989).
- [24] T. Senthil, M. Vojta, and S. Sachdev, Weak magnetism and non-Fermi liquids near heavy-fermion critical points, *Phys. Rev. B* **69**, 035111 (2004).
- [25] J. H. Pixley, R. Yu, and Q. Si, Quantum phases of the Shastry-Sutherland Kondo lattice: Implications for the global phase diagram of heavy-fermion metals, *Phys. Rev. Lett.* **113**, 176402 (2014).
- [26] D. Guerci, J. Wang, J. Zang, J. Cano, J. H. Pixley, and A. Millis, Chiral Kondo lattice in doped MoTe₂/WSe₂ bilayers, *Sci. Adv.* **9**, eade7701 (2023).
- [27] Ph. Nozières and A. Blandin, Kondo effect in real metals, *J. Phys. France* **41**, 193 (1980).
- [28] J. G. Rau and H.-Y. Kee, Symmetry breaking via hybridization with conduction electrons in frustrated Kondo lattices, *Phys. Rev. B* **89**, 075128 (2014).
- [29] P. Chandra, P. Coleman, and R. Flint, Hysteric order in the heavy-fermion compound URu₂Si₂, *Nature (London)* **493**, 621 (2013).
- [30] J.-X. Zhu, I. Martin, and A. R. Bishop, Kondo stripes in an Anderson-Heisenberg model of heavy fermion systems, *Phys. Rev. Lett.* **100**, 236403 (2008).
- [31] F. Mazza, P. Y. Portnichenko, S. Avdoshenko, P. Steffens, M. Boehm, E. S. Choi, M. Nikolo, X. Yan, A. Prokofiev, S. Paschen, and D. S. Inosov, Cascade of magnetic-field-driven quantum phase transitions in Ce₃Pd₂₀Si₆, *Phys. Rev. B* **105**, 174429 (2022).
- [32] D. M. Fobes, S. Zhang, S.-Z. Lin, P. Das, N. J. Ghimire, E. D. Bauer, J. D. Thompson, L. W. Harriger, G. Ehlers, A. Podlesnyak, R. I. Bewley, A. Sazonov, V. Hutanu, F. Ronning, C. D. Batista, and M. Janoschek, Tunable emergent heterostructures in a prototypical correlated metal, *Nat. Phys.* **14**, 456 (2018).
- [33] G. G. Marcus, D.-J. Kim, J. A. Tutmaher, J. A. Rodriguez-Rivera, J. O. Birk, C. Niedermeyer, H. Lee, Z. Fisk, and C. L. Broholm, Multi-*q* mesoscale magnetism in CeAuSb₂, *Phys. Rev. Lett.* **120**, 097201 (2018).
- [34] S. Jang, R. Kealhofer, C. John, S. Doyle, J.-S. Hong, J. H. Shim, Q. Si, O. Erten, J. D. Denlinger, and J. G. Analytis, Direct visualization of coexisting channels of interaction in CeSb, *Sci. Adv.* **5**, eaat7158 (2019).